



## Classification of natural circulation two-phase flow patterns using fuzzy inference on image analysis

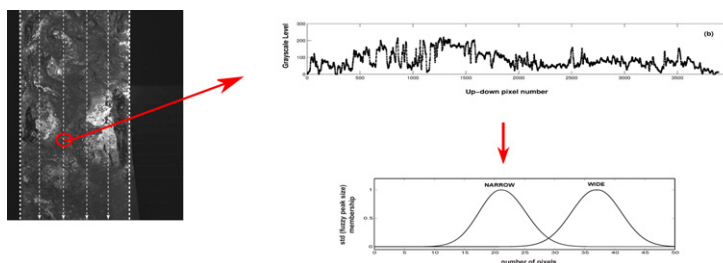
R.N. de Mesquita\*, P.H.F. Masotti, R.M.L. Penha, D.A. Andrade, G. Sabundjian, W.M. Torres, L.A. Macedo

Nuclear Engineering Center, Instituto de Pesquisas Energéticas e Nucleares, IPEN/CNEN, Av. Professor Lineu Prestes, 2242 Cidade Universitária, CEP 05508-000 São Paulo, Brazil

### HIGHLIGHTS

- ▶ A fuzzy classification system for two-phase flow instability patterns is developed.
- ▶ Flow patterns are classified based on images of natural circulation experiments.
- ▶ Fuzzy inference is optimized to use single grayscale profiles as input.

### GRAPHICAL ABSTRACT



### ARTICLE INFO

#### Article history:

Received 22 August 2011

Received in revised form 23 May 2012

Accepted 5 June 2012

### ABSTRACT

Two-phase flow on natural circulation phenomenon has been an important theme on recent studies related to nuclear reactor designs. The accuracy of heat transfer estimation has been improved with new models that require precise prediction of pattern transitions of flow. In this work, visualization of natural circulation cycles is used to study two-phase flow patterns associated with phase transients and static instabilities of flow. A Fuzzy Flow-type Classification System (FFCS) was developed to classify these patterns based only on image extracted features. Image acquisition and temperature measurements were simultaneously done. Experiments in natural circulation facility were adjusted to generate a series of characteristic two-phase flow instability periodic cycles. The facility is composed of a loop of glass tubes, a heat source using electrical heaters, a cold source using a helicoidal heat exchanger, a visualization section and thermocouples positioned over different loop sections. The instability cyclic period is estimated based on temperature measurements associated with the detection of a flow transition image pattern. FFCS shows good results provided that adequate image acquisition parameters and pre-processing adjustments are used.

© 2012 Elsevier B.V. All rights reserved.

### 1. Introduction

The new generation of nuclear power plant projects has included natural circulation as one of the main heat removal mechanisms for “loss of pump power” or “plant shutdown” accidents (Nayak and Sinha, 2007). In this regime, fluid circulation is mainly

caused by a driving force which arises from density differences due to temperature gradient. Natural circulation circuits have been used on chemical processes refrigeration, electronics, solar energy heating, nuclear energy and many other applications.

Many test facilities were built in order to study low pressure natural circulation in conditions related with reactors design, operational problems and their associated changes in flow patterns and hydro-dynamics. Boiling-water reactors development was one of the main causes for this study to happen. Two-phase flow patterns have been studied for many decades, and their related instabilities have been object of special attention recently. Many different instability categories have been established during this period both due to natural and forced two-phase circulation.

\* Corresponding author. Tel.: +55 11 31339420.

E-mail addresses: [rnavarro@ipen.br](mailto:rnavarro@ipen.br) (R.N. de Mesquita), [pmasotti@ipen.br](mailto:pmasotti@ipen.br) (P.H.F. Masotti), [rmpenha@ipen.br](mailto:rmpenha@ipen.br) (R.M.L. Penha), [delvonei@ipen.br](mailto:delvonei@ipen.br) (D.A. Andrade), [gdjian@ipen.br](mailto:gdjian@ipen.br) (G. Sabundjian), [wmtorres@ipen.br](mailto:wmtorres@ipen.br) (W.M. Torres), [lamacedo@ipen.br](mailto:lamacedo@ipen.br) (L.A. Macedo).

Natural circulation two-phase flow instabilities have been accepted to be classified as established by Delhaye in 1981 (Delhaye et al., 1981; Andrade et al., 2000; Nayak and Vijayan, 2008). These instabilities are usually divided into Type-I and Type-II groups, where the first group refers to gravity effects and was very important on SBWR (Simplified Boiling-Water Reactors) development (He and Edwards, 2008). Classical static phenomenon explains known bumping, geysering and chugging oscillations, which may couple to produce a repetitive behavior that not always is periodic. The term “chugging” is usually used to denominate the characteristic periodic expulsion of coolant from a flow channel (Bouré et al., 1973).

Recent improvements on image processing and acquisition technology made possible the discovery of new features and the detection of two-phase flow patterns through acquired digital images. Most of these studies have been looking for online detection and classification of flow patterns using digital processing resources (Crivelaro et al., 2002). As pressure drop from each phase is fundamentally dependent on void fraction values, flow parameters estimates and phase transitions characteristics are being pursued by many groups. Estimation of these features has been attained throughout the use of different artificial intelligence techniques.

A relation between flow type transitions and time-frequency covariances of void fraction signals was proposed by Selegim and Hervieu (1998) and neural networks have been used to detect phase transitions based on signal changes by Crivelaro et al. (2002). Improved image processing techniques (Hsieh et al., 1997; Shamoun et al., 1999; Maurus et al., 2002) and qualitative image analysis (Kirouac et al., 1999) have often been associated with other flow-measurement experimental techniques. Hot-wire anemometer (Zenit et al., 2001), conductivity probe (Yeoh et al., 2002), electrical-resistance-tomography (Dong et al., 2006), multiple-electrode impedance (He and Edwards, 2008), particle velocimetry (Fujiwara et al., 2004) and optical treatments (Ursenbacher et al., 2004; Wojtan et al., 2005) are other associated techniques used. The use of artificial intelligence techniques on these applications, can still be improved quantitatively and qualitatively in order to establish new database handling capabilities and to develop new flow-types detection methods. Precise prediction of flow-type transitions, void fraction, dry angles and other parameters are required by new two-phase flow heat transfer evaluation (Kattan et al., 1998a,b,c; Thome and El Hajal, 2003). Most of precedent work has been done on generic typical Steiner type flow map (Jassim et al., 2007).

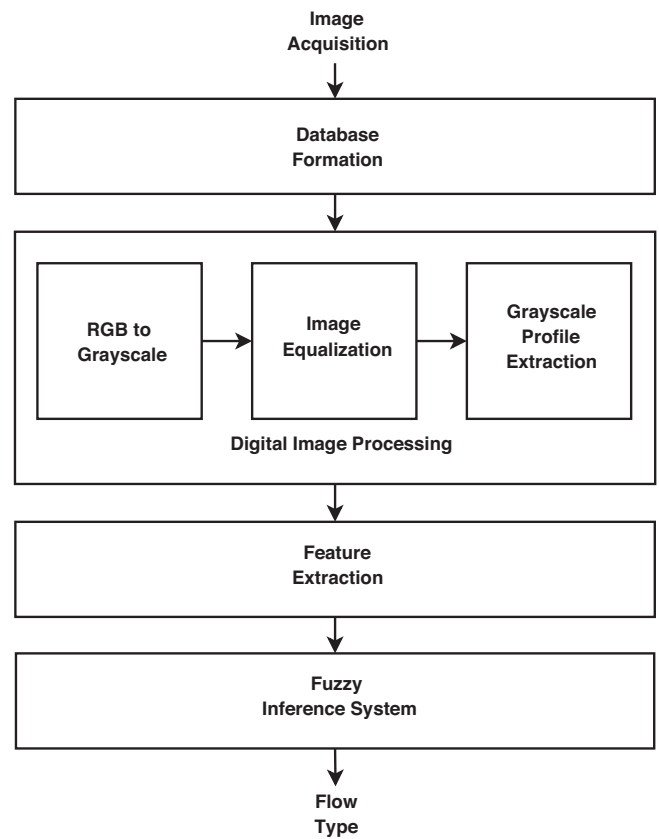


Fig. 1. Fuzzy Flow-type Classification System (FFCS) overall scheme.

This work proposes an automatic flow pattern recognition algorithm developed to detect chugging instability flow types observed on a natural circulation experimental loop, based on digital images acquired through a visualization section. Instability phase denominations are based on classical Bouré classification (Bouré et al., 1973). FFCS was created in order to demonstrate the importance and feasibility of implementing simple, fast (online) flow type identification systems using Fuzzy Inference Logic. FFCS was optimized to use as few fuzzy rules as possible. The rules were constructed based only on two main image extracted features. A previous work has described this system development initial steps (de Mesquita et al., 2010).

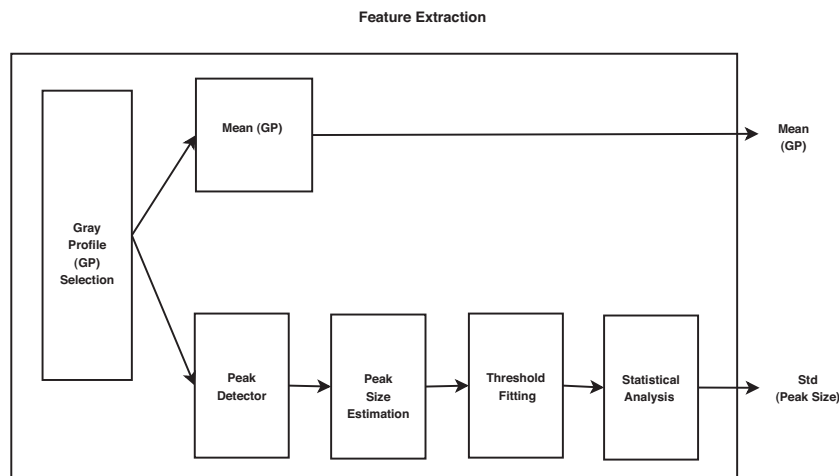


Fig. 2. Feature extraction module scheme.

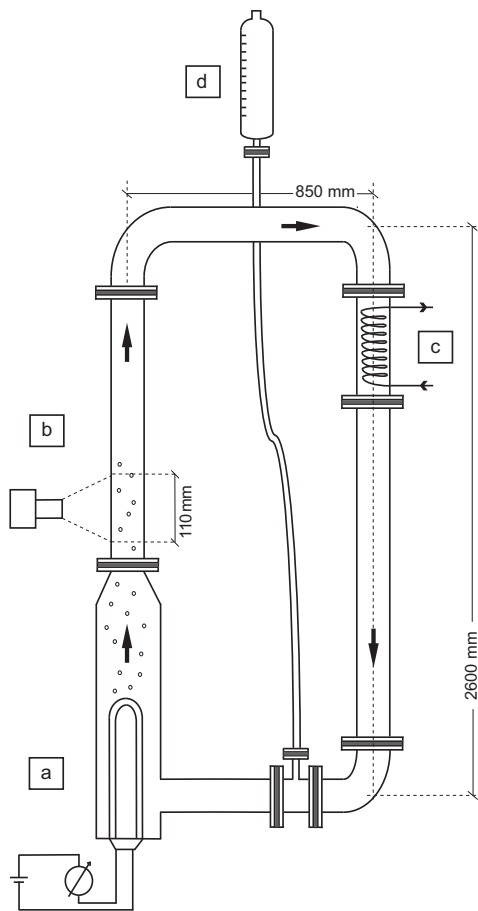


Fig. 3. Schematics of natural circulation loop facility with: (a) electrical heating section, (b) visualization section, (c) cooling section and (d) expansion tank.

## 2. Experimental setup and methods

### 2.1. Overall classification system

A representation of FFCS methodology is shown in Fig. 1, where a sequence of steps (database formation, image processing and feature extraction) precede Fuzzy Inference System (FIS) module. Feature extraction module is shown in Fig. 2, where feature extraction steps are represented. The two selected features are: mean of grayscale level profile (mean(GP) or MGP) and standard deviation of grayscale profile peak sizes (std(peak size) or STDPS), which will be further explained on this text.

### 2.2. Natural circulation glass loop

The Natural Circulation Facility (NCF) (Fig. 3) installed at *Instituto de Pesquisas Energéticas e Nucleares, IPEN/CNEN*, is an experimental circuit designed to provide thermal hydraulic data related to one and two phase flow under natural circulation conditions.

NCF is a rectangular assembly (with 2600 mm height and 850 mm width) of borosilicate glass tubes that are temperature resistant, with 38.1 mm internal diameter and 4.42 mm wall-thickness each. The loop has a heated section (Fig. 3(a)), also made of glass tube with 76.2 mm internal diameter and 880 mm length. This section has two Ni–Cr alloy electric heaters (H1 and H2) in U form and stainless steel clad. Electric power in H1 can be adjusted in a 0–100% range by an autotransformer. The heaters are composed of electrical resistors that can deliver up to 8000 W. The H2 heater operates at constant power. The cooling section (Fig. 3(c))

consists of a heat exchanger/condenser, also made of glass, with two internal spiral coils where tap water flows. Cooling water at ambient temperature is pumped from a 2 m<sup>3</sup> reservoir to the heat exchanger/condenser with the desired cooling flow rate being measured by two rotameters. Circuit has an expansion tank (Fig. 3(d)) opened to atmosphere in order to accommodate fluid level changes due to the temperature and void fraction changes. This tank is connected to the circuit through a flexible tube at its lower region in order to prevent steam entrance (Andrade et al., 2000). Approximately 12 l of demineralized water are used to fill the circuit.

Fifteen 1.5 mm K-type (Chromel–Alumel) ungrounded thermocouples are distributed along the circuit to measure fluid and ambient temperatures. Three K-type thermocouples with exposed junction are attached to the glass tube wall at the circuit hot leg. Two Validyne differential pressure transducers are used to measure the relative pressure at the heaters outlet and the water level in the expansion tank. All instruments were calibrated in laboratory. A data acquisition system assembled with SCXI series equipment from National Instruments is used to acquire sensor data. Visualization is possible in all regions of the circuit, and a visualization section with a CCD (charged-couple device) camera was adjusted with backlight illumination (Fig. 3(b)). Temperature measurements and image acquisition were concomitantly done in order to characterize phase transition patterns and correlate them with the periodic static instability (chugging) measured cyclic period.

Chugging instability cycles are usually divided in three different phases called incubation, expulsion and refill periods (Delhaye et al., 1981; Andrade et al., 2000; Nayak and Vijayan, 2008). They are considered relaxation instabilities characterized by periodic expulsion of coolant from the channel. The experiments were adjusted to sustain a cyclic and periodic behavior of this instability.

The incubation phase has no net flow at the loop when vapor bubbles grow in number and size and vapor remains at upper horizontal leg. At this phase, the circuit pressure grows slightly expelling the liquid from the cold leg to the expansion tank (Fig. 3(d)). The slug flow is replaced by churn flow at the called expulsion phase, when liquid entrained by vapor is expelled from hot leg. The expansion tank level arises to its maximum value. The final phase is characterized by the inversion of flow rate direction caused by the difference of hydrostatic head, replacing the hot water at the heater by cold water coming from coil cooler. The vapor production at the heater decreases and the horizontal part of the hot leg is filled with water again, beginning the overall cycle once more (Andrade et al., 2000). This periodic flow oscillation behavior can be observed thoroughly in this facility due its glass-made tubes transparency.

### 2.3. Image acquisition setup

Image acquisition was done simultaneously with temperature measurements using high resolution digital camera with 250  $\mu$ s shutter speed. Lens mount were configured to enable macro focus and image acquisition was done at one frame per second rate during different cycles of 1000–1500 s long. Typical acquisition modes generated 3888  $\times$  2592 pixels frames at longitudinal tube section with a resolution of approximately 0.03 mm/pixel. Backlight illumination technique showed to be the optimal condition to obtain image borders best definition. Images were acquired at an approximate 120 mm longitudinal section of the cylindrical hot leg tube (46.3 mm external diameter) shown in Fig. 3(b).

### 2.4. Image patterns characterization

Image database was organized based on three main chugging subtypes, incubation (I), expulsion (E) and refill (R). Temperature measurements of a typical NCF two-phase flow experiment are

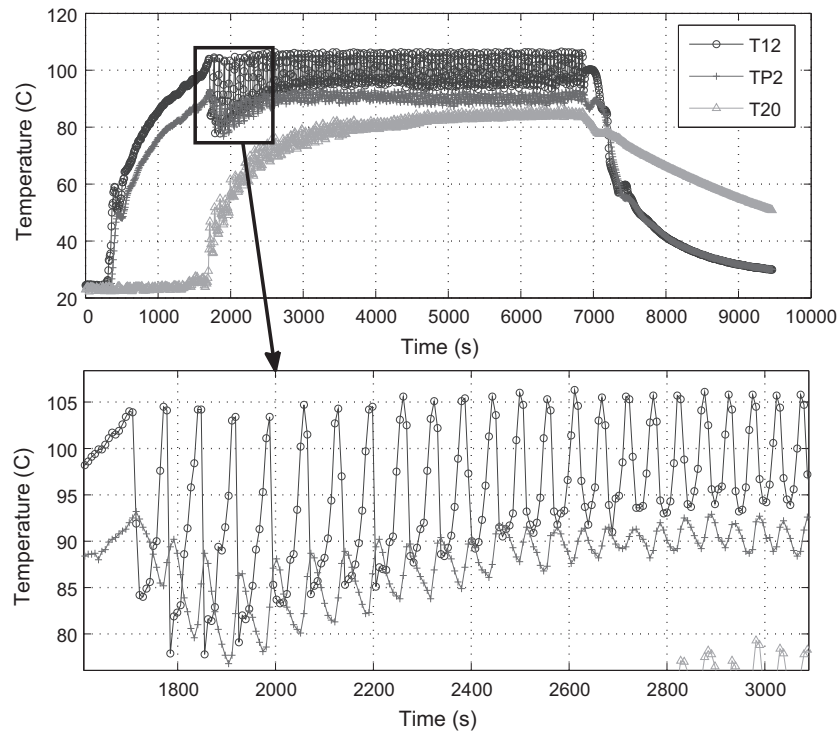


Fig. 4. Temperature cyclic periodic behavior through time on a natural circulation facility two-phase flow instability (chugging) experiment.

shown in Fig. 4. Patterns images were acquired simultaneously with circuit temperature measurements synchronized in time. The heating power was estimated to be raised up to 7270 W with an ambient temperature of 25 °C. Cooling flow rates of 140 l/h were kept constant during the approximate 9500 s experiment. Periodic behavior was confirmed by the detection of the refill-to-incubation phase transition image pattern (Fig. 5). This detection is described with more detail elsewhere (Andrade et al., 2000; de Mesquita et al., 2010).

The instability two-phase flow cyclic behavior can be observed through temperature measurements and by cyclic flow pattern detection time interval. A regular  $T$  period of 49 s for a complete chugging cycle is estimated after stabilization (Fig. 4) occurs. The cycle is composed of an incubation phase ( $T$  to  $(T+30)$  s), an expulsion phase ( $(T+30)$  s to  $(T+35)$  s) and a refill phase which lasts for the remaining 14 s of the cycle period.

The image database (Fig. 1) was composed of selected images related to each subtype phase of chugging cycle. Images acquired at moments corresponding to the center region of each instability phase time-intervals were selected in order to adjust the classification system. Images corresponding to periods near to instability flow subtype transitions were not considered on this work in order to best estimate the fuzzy classification ability. From 2530 images, 32 sample images were selected to characterize each flow subtype. The images in Fig. 8 show four examples for each chugging subtype. From these images is possible to note that there are visual similarities and differences among the same subtype examples.

### 2.5. Digital image processing

Image database was composed of 96 full-sized  $10^7$  pixels “rgb” images (red-green-blue pattern) in compressed image files formats (ISO/IEC 10918-4:1999) organized in three subtype classes in order to adjust FIS parameters. The digital image processing (DIP) algorithm module was composed of a consecutive set of Matlab (MATLAB, 2010) functions (Fig. 1) An interpolating gray-level

transforming function (*rgb2gray*) produces a grayscale image as output. The following function is a histogram equalization function (*imadjust*) which maps the values in intensity image to new values in such that 1% of data is saturated at low and high intensities of this image. After these two steps, a line extraction algorithm is



Fig. 5. Characteristic image of periodic transition from refill-to-incubation phase in ascending flow of a chugging instability.

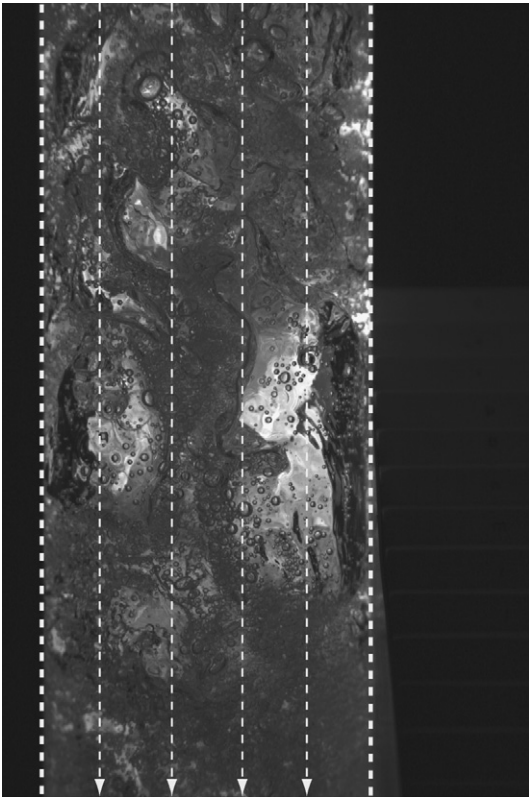


Fig. 6. Up-down grayscale profiles and cropping sections.

applied in order to obtain grayscale profiles. From each sample, four longitudinal (top-down) and equidistant (inside tube) lines of 3888 pixels (Fig. 6) were extracted. Acquired images originally included (inside the visual field frame) a focus calibration pattern beside the tube (Fig. 6). This pattern was used to measure the field depth and the distance from the camera to the glass tube surface.

## 2.6. Image feature extraction

The feature extraction (FE) module (Fig. 2) is composed of functions applied solely on one vertical grayscale profile line each time (second or third lines). This choice was based on optimization through testing the system with different combinations of profiles. Typical vertical grayscale profiles related to each flow-type are shown in Fig. 7.

A subsequent step inside FE module smooths grayscale profiles in order to obtain meaningful information from posterior peak detector. A “peak and valley” algorithm is then applied, in order to obtain peak sizes and the number of peaks relative to different peak-to-peak thresholding levels. At first, gray intensity level ( $I$ ) variation is obtained by subtracting  $I(t) - I(t - 1)$ , where  $t$  is the pixel number. Gray intensity level variation contains information about image borders on small scale. Most of images analyzed had high density of bubbles with different sizes. Peak sizes are given in number of pixels unit. Each grayscale profile had different peak sizes distribution. Profiles that had wider peaks were related to images with higher contrast steps. Thresholding level was used as one of our free parameters adjustment in order to obtain the best classification. Standard deviation of gray-level profile peak size (STD(GP)) was one chosen extracted feature. The other chosen feature was the simple mean of grayscale level profile (MGP). Feature choice was done observing many different features and comparing their distribution over chugging instabilities flow subtype regions. Some of these image samples are shown in Fig. 8.

## 2.7. Fuzzy inference system

A fuzzy inference system (FIS) is an inference system based on Fuzzy Logic (Zadeh, 1965) that uses linguistic expressions to compose a set of rules describing a method for inferring conclusions or obtaining results, based on a set of input data. On a classification task, FIS is based on extracted features from data that best represents and differentiates a data class from the other. These systems are usually described to map “crisp” inputs into “crisp” outputs and are composed by four basic components: rules, *fuzzifier*, inference engine and *defuzzifier* (Mendel, 1995). As a product of the system of rules using fuzzy variables, a non-linear mapping is obtained and can be expressed as a function  $y=f(x)$ . This mapping can be

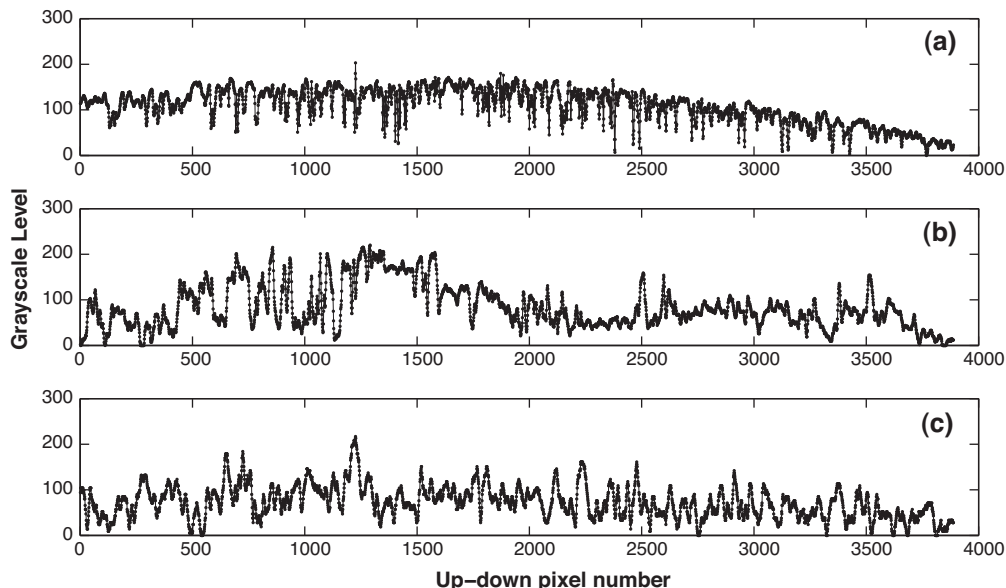
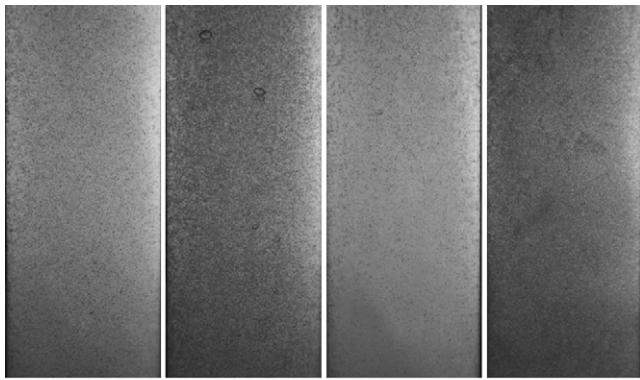
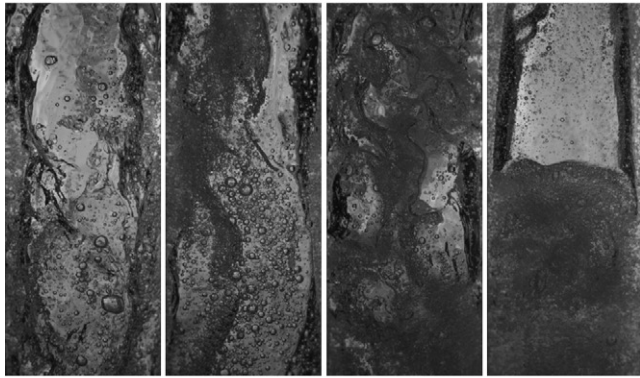


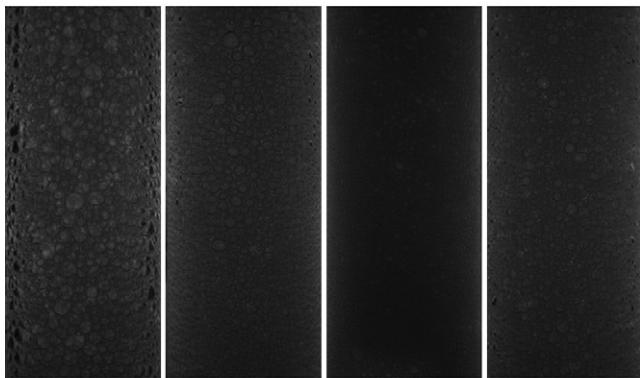
Fig. 7. Up-down grayscale profiles for different chugging phases: (a) incubation, (b) expulsion and (c) refill.



(a) I8884 (b) I9062 (c) I9239 (d) I9257



(e) E8812 (f) E8901 (g) E9070 (h) E9156



(i) R8821 (j) R9084 (k) R9236 (l) R9324

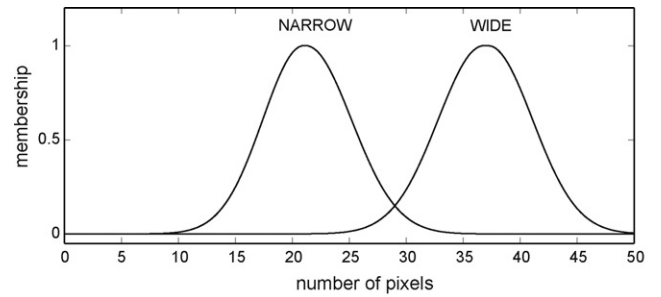
**Fig. 8.** (a–d) Incubation (I), (e–h) expulsion (E) and (i–l) refill (R) cropped image samples.

described as a relation between fuzzy sets. A fuzzy set  $F$  in  $U$  may be represented as a set of ordered pairs of a generic element  $x$  and its grade of membership  $\mu_F(x)$ :

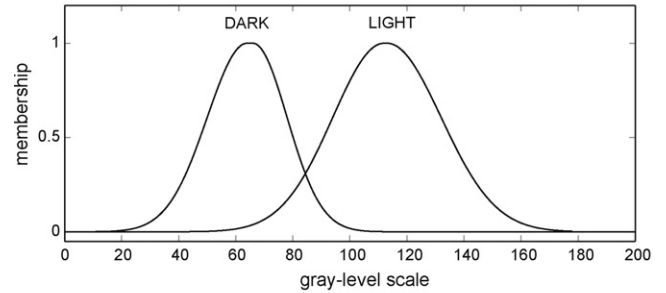
$$F = \{(x, \mu_F(x)) | x \in U\} \quad (1)$$

whether  $U$  is discrete or continuous,  $F$  is commonly written as:

$$F = \sum_U \frac{\mu_F(x)}{x} \quad (2)$$



(a) Standard Deviation of Grayscale Profile Peak Sizes (STDPS)



(b) Mean of Grayscale Level Profile (MGP)

**Fig. 9.** Fuzzy Flow-type Classification System (FFCS) input membership functions: (a) standard deviation of grayscale profile peak sizes (STDPS) and (b) mean of grayscale level profile (MGP).

or,

$$F = \int_U \frac{\mu_F(x)}{x} \quad (3)$$

where the summation and integral symbols describes the union of all points  $x \in U$  with  $\mu_F(x)$  membership.

The *fuzzification* will map a collection (col) of “crisp” points (real or integer numbers) into a fuzzy set  $\hat{A}$  in  $U$ , which can be usually represented as a fuzzy membership function associated with  $x$ , attributing different membership values representing the *true-ness* of pertinence of each  $x$  to set  $\hat{A}$ . This membership functions assume different types and shapes. In this work we used Gaussian membership functions (see Fig. 9).

Each Fuzzy rule is usually based on a “IF-THEN” sentence that has a membership value between 0 and 1. The sentence “IF  $u$  is  $A$ , THEN  $v$  is  $B$ ”, where  $u \in U$  and  $v \in V$  has a membership value represented by:

$$\mu_{(A \rightarrow B)}(x, y) \in [0, 1] \quad (4)$$

The inference engine is evaluated combining IF-THEN rules based on fuzzy input sets in  $U: U_1 \times U_2 \times \dots \times U_p$  to output sets in  $V$ , where  $p$  is the size of each discrete universe of discourse associated with each rule which is interpreted as a fuzzy implication. Using a discrete collection of data, each rule can be represented as:  $\mu_{(B^l)}(y) = \mu_{(A_x)} \circ R^l(y)$  or,

$$\mu_{(B^l)}(y) = \max_{(x \in A_x)} [\mu_{(A_x)} * \mu_{(A \rightarrow B)}(\bar{x}, y)] \quad (5)$$

where the symbol  $\circ$  denotes fuzzy set composition,  $\max$  is the maximum operator, and  $*$  is any t-conorm operator used for fuzzy set intersection. All these logical operations are used to aggregate the different rules and quantify trueness values for each rule and for its consequent part. The inference then is done obtaining a final value for inferred outputs.

**Table 1**  
Classification outcome rates.

Instability type	2nd line	3rd line
Incubation	93.75%	68.75%
Expulsion	87.50%	84.38%
Refill	90.63%	90.63%
Total (1+E+R)	90.63%	81.25%

The final fuzzy set  $B = A_x \circ [R^{(1)}, R^{(2)}, \dots, R^{(M)}]$  determined by all the rules in the rule base, combining all  $B^l$  and its associated membership function  $\mu_{(A_x)} \circ R^l(y)$  for all  $l = 1, 2, \dots, M$  (Mendel, 1995).

For a Gaussian membership function for  $\mu_x$ , where all input points for each input variable have the same level of uncertainty, the spreads of the input sets will be the same, in which case  $\sigma_{(x_k)}^2$  is a constant. The  $k$ th input fuzzy set and the corresponding rule antecedent fuzzy sets are assumed to have the following forms:

$$\mu_{(x_k)} = \exp \left\{ \left( -\frac{1}{2} \right) \left[ \frac{(x_k - m_{(x_k)})}{\sigma_{(x_k)}} \right]^2 \right\} \quad (6)$$

Assuming the mean of the fuzzy input sets to be  $m_{(x_k)}$ , the crisp measured input,  $x_k^l$  can be seen as a noisy data pre-filtered by Gaussian inference. Finally, for a system based on non-singleton fuzzification, max-product composition, max-product inference, and Gaussian membership functions,  $y$  can be written as a non-linear function of  $x$  by:

$$y = f(x) = \sum_{l=1}^M y^l \phi_l(x) \quad (7)$$

where  $\phi_l(x)$  are called fuzzy basis functions for non-singleton fuzzification, where  $l = 1, 2, \dots, M$ . Fuzzy Inference System can then be referred as a fuzzy basis function expansion (Wang, 1992; Mendel, 1995).

### 2.8. Fuzzy Flow-type Classification System

The fuzzy flow-type classification system (FFCS) was implemented using Fuzzy Matlab Toolbox (MATLAB, 2010) where two selected image features were used as Gaussian membership inputs: standard deviation of grayscale profile peak sizes (STDPS) (Fig. 9(a)) and the simple mean of each grayscale profile (mean of grayscale level profile (MGP)) (Fig. 9(b)). FFCS overall classification was implemented in this work based on a simple Mamdani inference type system (Esragh and Mamdani, 1981) using three basic rules. The implication was optimized through the following rules:

- Rule 1: If MGP is DARK and STDPS is NARROW then flow-type is R;  
 Rule 2: If MGP is LIGHT and STDPS is NARROW then flow-type is I;  
 Rule 3: If MGP is LIGHT and STDPS is WIDE then flow-type is E.

### 3. Results

The results of tests made with FFCS are shown in Table 1.

FFCS showed good results to the sampling method described in Section 2.4 as can be seen in Table 1. The right classification rates corresponding to each instability type and the total classification rate are presented in table first column. These rates were obtained using the second up-down grayscale profile as can be seen in Fig. 6. In the second column the classification rates obtained applying FFCS to third up-down grayscale profile are shown. Best classification rates would have been obtained if more specific and uniform patterns were used as input to FFCS. System generalization capability was stressed to its limit by using a testing set composed of significant variations of subtype typical flow-patterns (Fig. 8).

Fuzzy membership functions were constructed based on chosen features distribution over individual grayscale lines. Superposition of two grayscale vertical lines did not present improvements on classification task.

### 4. Conclusions

These results show that it is possible to implement image pattern classification systems based on simple features using a fuzzy inference system, provided that proper image processing is done. FFCS was based on single grayscale profiles, which allows its usage on line-scan camera image acquisition systems. Fuzzy systems have a real advantage over other artificial intelligence methods, as they allow expert knowledge to be explicitly included on inference rules. This property can be read directly over the rule base and membership functions definition. Among the different features tried on this work, peak-size distribution (STDPS) and grayscale level mean (MGP) showed to be the best features. A comprehension of these features predominance can be investigated by looking directly into subtype typical images (Fig. 8). These features may be used as a first step to elaborate new models able to extract useful information based on high void fraction two-phase flow visualization.

### Acknowledgements

The authors wish to acknowledge the support for this work by the Department of Chemical Engineering of the Polytechnic School of the University of São Paulo.

### References

- Andrade, D.A., Belchior Jr., A., Sabundjian, G., Bastos, J.L.F., 2000. Two-phase instabilities in a natural circulation rectangular loop. In: Proc. 8th International Conference on Nuclear Engineering, Baltimore, MD.
- Bouré, J.A., E., B.A., Tong, L., 1973. Review of two-phase flow instability. Nucl. Eng. Des. 25, 165–192.
- Crivelaro, K.C.O., Selegim Jr., P., Hervieu, E., 2002. Detection of horizontal two-phase flow patterns through a neural network model. J. Braz. Soc. Mech. Sci. 24 (1), 70–75.
- de Mesquita, R.N., Penha, R.M.L., Masotti, P.H.F., Sabundjian, G., Andrade, D.A., Umbehaun, P.E., Torres, W.M., Conti, T.N., Macedo, L.A., 2010. Two-phase flow patterns recognition and parameters estimation through natural circulation test loop image analysis. In: Proc. 7th ECI International Conference on Boiling Heat Transfer 2009, Curran Associates, Inc., Florianopolis, Santa Catarina, Brazil.
- Delhaye, J.M., Giot, M., Riethmuller, M.L., 1981. Thermohydraulics of Two-Phase Systems for Industrial Design and Nuclear Engineering. McGraw-Hill, New York (Chap. 17).
- Dong, F., Xu, Y., Hua, L., Wang, H., 2006. Two methods for measurement of gas-liquid flows in vertical upward pipe using dual-plane ert system. IEEE Trans. Instrum. Meas. 55, 1576–1586.
- Esragh, F., Mamdani, E.H., 1981. A general approach to linguistic approximation. In: Fuzzy Reasoning and Its Applications. Academic Press, London.
- Fujiwara, A., Minato, D., Hishida, K., 2004. Effect of bubble diameter on modification of turbulence in an upward pipe flow. Int. J. Heat Fluid Flow 25, 481–488.
- He, W., Edwards, R.M., 2008. Stability analysis of a two-phase tested loop. Ann. Nucl. Energy 35, 525–533.
- Hsieh, C.C., Wang, S.B., Pan, C., 1997. Dynamic visualization of two-phase flow patterns in a natural circulation loop. Int. J. Multiphase Flow 23 (6), 1147–1170.
- Jassim, E.W., Newell, A.T., Chato, J.C., 2007. Probabilistic determination of two-phase flow regimes in horizontal tubes utilizing an automated image recognition technique. Exp. Fluids 42, 563–573.
- Kattan, N., Thome, J.R., Favrat, D., 1998a. Flow boiling in horizontal tubes. Part 1. Development of a diabatic two-phase flow pattern map. J. Heat Transfer 120 (1), 140–147.
- Kattan, N., Thome, J.R., Favrat, D., 1998b. Flow boiling in horizontal tubes. Part 2. New heat transfer data for five refrigerants. J. Heat Transfer 120 (1), 148–155.
- Kattan, N., Thome, J.R., Favrat, D., 1998c. Flow boiling in horizontal tubes. Part 3. Development of a new heat transfer model based on flow pattern. J. Heat Transfer 120 (1), 156–165.
- Kirouac, G.J., Trabold, T.A., Vassallo, P.F., Moore, W.E., Kumar, R., 1999. Instrumentation development in two-phase flow. Exp. Therm. Fluid Sci. 20, 79–93.
- MATLAB, 2010. MATLAB, version 7.10.0 (R2010a). The MathWorks, Inc., Natick, MA.
- Maurus, R., Ilchenko, V., Sattelmayer, T., 2002. Study of the bubble characteristics and the local void fraction in subcooled flow boiling using digital imaging and analyzing techniques. Exp. Therm. Fluid Sci. 26, 147–155.

- Mendel, J.M., 1995. Fuzzy logic systems for engineering: a tutorial. *Proc. IEEE* 83, 345–437.
- Nayak, A.K., Sinha, R.K., 2007. Role of passive systems in advanced reactors. *Prog. Nucl. Energy* 49, 486–498.
- Nayak, A.K., Vijayan, P.K., 2008. Flow instabilities in boiling two-phase natural circulation systems: a review. *Sci. Technol. Nucl. Install.* 2008, 1–15.
- Seleglim Jr., P., Hervieu, E., 1998. Direct imaging of two-phase flows by electrical impedance measurements. *Meas. Sci. Technol.* 9, 1492–1500.
- Shamoun, B., Beshbeeshy, M.E., Bonazza, R., 1999. Light extinction technique for void fraction measurements in bubbly flow. *Exp. Fluids* 26, 16–26.
- Thome, J.R., El Hajal, J., 2003. Two-phase flow pattern map for evaporation in horizontal tubes: latest version. *Heat Transfer Eng.* 24 (6), 3–10.
- Ursenbacher, T., Wojtan, L., Thome, J.R., 2004. Interfacial measurements in stratified types of flow. Part I. New optical measurement technique and dry angle measurements. *Int. J. Multiphase Flow* 30, 107–124.
- Wang, L.X.M.J., 1992. Fuzzy basis functions, universal approximation, and orthogonal least squares learning. *IEEE Trans. Neural Netw.* 3, 807–813.
- Wojtan, L., Ursenbacher, T., Thome, J.R., 2005. Measurements of dynamic void fractions in stratified types of flow. *Exp. Therm. Fluid Sci.* 29, 383–392.
- Yeoh, G.H., Tu, J.Y., Lee, T., Park, G.C., 2002. Prediction and measurement of local two-phase flow parameters in a boiling flow channel. *Numer. Heat Transfer A* 42, 173–192.
- Zadeh, L.A., 1965. Fuzzy sets. *Inform. Control* 8, 338–353.
- Zenit, R., Koch, D.L., Sangani, S., 2001. Measurements of the average properties of a suspension of bubbles rising in a vertical channel. *J. Fluid Mech.* 429, 307–342.